Quasiparticle interferometer controlled by quantum-correlated Andreev reflection

Hayato Nakano and Hideaki Takayanagi
NTT Basic Research Laboratories, Midori-cho 3-9-11, Musashino-shi, Tokyo 180, Japan
(Received 24 June 1992; revised manuscript received 29 October 1992)

We propose a quasiparticle interferometer and give a theoretical analysis for it. It consists of a Josephson junction (JJ) and a Y junction composed of normal-electron waveguides. The interferometer should enable us to confirm experimentally the phase interaction between a quasiparticle and a superconducting state at the superconductor–normal-metal (SN) interface. This interaction is caused by Andreev reflection. The supercurrent through the JJ modifies, by Andreev reflection, the interference of a quasiparticle in the waveguide and affects the normal resistance of the waveguide. The dependence of the resistance on the phase difference of JJ is determined by the characteristics of the Y junction and the normal reflection at the SN interface.

I. INTRODUCTION

Recent research on various mesoscopic systems has provided us with many new viewpoints on the phase-coherence phenomena of electrons.[1] This coherence is attributed to the microscopic quantum states of a single quasiparticle, i.e., an electron or a hole. On the other hand, research on phase-coherence phenomena in superconducting states has a long history and has already been applied to devices such as SQUID.[2] This coherence is, of course, a well-known property of the macroscopic quantum state.

One of the most interesting topics beyond mesoscopic physics is the problem of the relationship between the microscopic "phase" of a normal electron and the macroscopic "phase" of a superconducting state. We should be able to clarify this problem by considering a normal-metal–superconductor coupled system. Is the coupled system a "microscopic" quantum system, a "macroscopic" quantum system, both, or neither?

In this article, we investigate the microscopic quantum-mechanical aspect of the coupled system. The most important phenomenon which combines the macroscopic phase and the microscopic phase, is Andreev reflection which occurs at the superconductor–normal-metal (SN) interface.[3] It is expected that an Andreev-reflected quasiparticle in the normal region would be phase-shifted by the macroscopic phase of the superconductor.[4] Recently, we have proposed a quasiparticle interferometer which enables us to confirm experimentally the phase interaction.[5] In this paper we give a more detailed analysis of the interferometer and discuss its various characteristics.

The plan of the paper is as follows. In Sec. II, we review the theory of Andreev reflection, focusing on the phase interaction between a quasiparticle in a normal metal and a superconducting state. In Sec. III, we summarize our proposal for a quasiparticle interferometer controlled by Andreev reflection, and briefly discuss the qualitative behavior of the interferometer. In Sec. IV, we give a quantitative analysis of the interferometer for simple cases, which includes some important effects, for example, the normal reflection at the SN interface. Finally, in Sec. V we discuss on the results of Sec. IV.

II. PHASE INTERACTION DUE TO ANDREEV REFLECTION

Consider the situation shown in Fig. 1. A normal metal is in contact with a superconductor at $x=0$. Neglecting the penetration of the superconducting pair potential into the normal region, we assume the steplike pair potential

$$\Delta(\mathbf{r})=\begin{cases}0 & \text{for } x<0 \text{ normal metal },\\ \Delta_0 e^{i\theta} & \text{for } x>0 \text{ superconductor },\end{cases} \tag{2.1}$$

where θ is the macroscopic phase of the superconductor. The wave functions in this system can be obtained in terms of the two-component representation by solving the Bogoliubov–de Gennes equation.[6] For simplicity, we treat the case where there is no *intrinsic* normal reflection at the SN interface. The effect of intrinsic normal reflection will be discussed in Sec. IV. In that case, when an electron is incident from the left, it is Andreev-reflected, changes into a hole, and then returns to the left. This process is expressed by the wave function in the normal-metal region as $\psi=\psi_{\rm inc}+\psi_{\rm ref}$,[7] where

$$\psi_{\rm inc}=\begin{bmatrix}1\\0\end{bmatrix}\exp[i(q^+x+\mathbf{q}_\perp\cdot\mathbf{r}_\perp)] , \tag{2.2a}$$

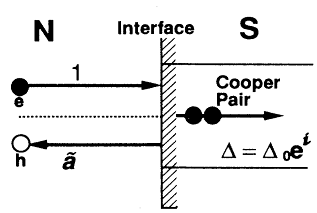

FIG. 1. Simple configuration for Andreev reflection. The Andreev-reflected hole is phase-shifted by the macroscopic phase of the superconductor.

$$\psi_{\rm ref}=\tilde{a}\begin{bmatrix}0\\1\end{bmatrix}\exp[i(q^{-}x+\mathbf{q}_{\perp}\cdot\mathbf{r}_{\perp})] \; . \tag{2.2b}$$

These are the incident electron and the Andreev-reflected hole, respectively. Here, $q^{\pm}$ is the wave number for the direction perpendicular to the interface given by

$$q^{\pm}=(2m/\hbar^2)^{1/2}(E_F-E_{\perp}\pm E)^{1/2} \; , \tag{2.3}$$

where m and E_F are the electron effective mass and the Fermi energy in the normal metal, and $\mathbf{q}_\perp$ is the transverse wave number, which gives $E_\perp=(\hbar^2/2m)\mathbf{q}_\perp^2$, and E is the excitation energy measured from the Fermi energy. It should be noted that when the incident energy is zero, the wave number of the Andreev-reflected hole is time reversed to that of the incident electron, and the hole traces back over the same path as the incident electron. We call this property "retroactive."

When the energy is within the superconducting gap energy Δ_0, the electron is perfectly Andreev-reflected, and thus changes into a hole. A simple calculation gives the Andreev reflection coefficient $\tilde{a}$:

$$\tilde{a}=e^{-i(\varphi+\theta)} \; , \tag{2.4}$$

where

$$\varphi=\arctan\sqrt{(\Delta_0/E)^2-1} \; . \tag{2.5}$$

Because the probability amplitude of the Andreev-reflected hole is $\tilde{a}^*\tilde{a}=1$, a single hole returns when a single electron is incident. Therefore, under the Andreev reflection, the net charge $2e$ is transferred for the incidence of the charge e. This phenomenon is called the "excess current" and causes the full half reduction in the normal resistance of the system which contains the SN interface.

The excess current is one important aspect of Andreev reflection, and it has already been mentioned often and is widely observed. The other important aspect is the phase shift by Andreev reflection. As seen in Eq. (2.4), an Andreev-reflected hole is phase-shifted by the macroscopic phase of the superconductor θ. When a hole is incident, it is phase shifted in the same way by Andreev reflection and changes into an electron. This aspect of Andreev reflection has rarely been referred to and has never been confirmed experimentally.

We close this section by emphasizing that the phase shift $\varphi+\theta$ by Andreev reflection does not depend upon $\mathbf{q}_\perp$, that is, it is independent of the incidence angle for the interface. In the following section,we propose a quasiparticle interferometer which should enable us to examine experimentally this phase interaction.

III. THE QUASIPARTICLE INTERFEROMETER CONTROLLED BY ANDREEV REFLECTION

The above phase shift by Andreev reflection cannot be observed in a single SN geometry because only the reflection probability that has lost the phase information can be observed. Some ideas for the observation of this phase shift have been proposed.[8–10] Al'tshuler, Khmelnitskii, and Spivak,[8] and Al'tshuler and Spivak[9] paid attention to the modification of the weak localization and conductance fluctuation by Andreev reflection. These phenomena occur by means of the quantum interference, in the same way the behavior of our interferometer described below. Their interference is, however, governed by random scatterers and is uncontrollable. Therefore, the proposed observations are indirect. Büttiker and Klapwijk[10] proposed to observe the transition of the flux quantum from the superconducting state to the normal one. This transition occurs through the phase interaction by Andreev reflection. In this experiment one must apply a magnetic field to a very small ring, and it should affect the superconductivity itself. So, it might be difficult to ascertain that the result of the experiment is due to the phase interaction.

An interferometer structure must be formed in order to confirm directly the phase interaction. Figure 2 shows our proposed interferometer.[5] It consists of a Josephson junction (JJ) and a Y-type junction composed of normal-electron waveguides. The first branch of the Y junction is the entrance for the incident electron or hole. The second branch is in contact with an electrode of the JJ, and the third branch is in contact with the other electrode; these contacts constitute the SN interfaces where Andreev reflections occur. The length L of these two branches must be shorter than the phase coherence length L_ϕ of the waveguide, so that an electron or hole conserves its phase memory during the round trip between the Y-junction point and the SN interface.

Let us focus on the resistance between the first branch of the Y junction (Q) and an electrode of the JJ (P). The ordinary resistance R_N across Q-P is determined by the reflective characteristics of the Y junction or a constriction on branch Q. It is usually of the order of h/e^2.

An electron wave incident from Q is divided between the second and third branches. Each partial electron wave propagates along a waveguide branch, reaches the SN interface, and is then Andreev-reflected. The Andreev reflection phase shifts the partial hole wave by the macroscopic phase of the electrode, θ_1 or θ_2. Andreev-reflected partial hole waves return along the original partial electron's paths and meet again at the Y-junction point. The phase advances during the round trip cancel

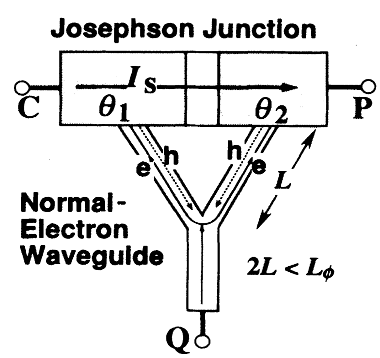

FIG. 2. The proposed quasiparticle interferometer. We focus on the resistance across Q-P, which varies as a function of the supercurrent flowing in the Josephson junction.

out because of the retroactive property of Andreev-reflected holes. Thus, the phase difference when two partial hole waves meet is exactly determined by the phase shifts they undergo when they are Andreev-reflected, that is, $\theta_1-\theta_2$. By interference, a proportion $\frac{1}{2}[1+\cos(\theta_1-\theta_2)]$ of the holes is received by the first branch, and this amount contributes as the excess current, resulting in a decrease in the resistance across Q-P. Therefore, the phase difference of the JJ changes the resistance across Q-P, and the conductance G_{QP} is estimated by

$$G_{QP}=\frac{1}{R_N}[1+\cos(\theta_1-\theta_2)] \ . \tag{3.1}$$

Thus, the setup works as an interferometer. This is, however, just a qualitative estimate and the quantative analysis is given in the next section.

The phase difference $\theta_1-\theta_2$ between two electrodes of a JJ varies with the supercurrent I_s flowing through the JJ. The relationship is given by

$$I_s=I_0\sin(\theta_1-\theta_2) \ , \tag{3.2}$$

where I_0 is the critical current of the JJ.[11] Therefore, the phase difference can be controlled from $-\pi/2$ to $\pi/2$ by changing the bias supercurrent from $-I_0$ to I_0. Consequently, the differential resistance across Q-P varies from $\frac{1}{2}R_N$ to R_N by Eq. (3.1) as a function of the bias supercurrent of the JJ. Observation of this phenomenon experimentally would confirm the phase interaction between a quasiparticle and a superconducting state.

IV. QUANTITATIVE ANALYSIS OF THE INTERFEROMETER

A. Models of analysis

In the previous section we gave a basic explanation of our interferometer. Now, we give a more detailed analysis. For simplicity, we limit our analysis to cases where the normal-electron waveguide is operated in a single mode. The wave function in each branch j of the waveguide is then expressed as the superposition of four linearly independent solutions of the Bogoliubov–de Gennes equation: incoming electron and hole waves, and outgoing electron and hole waves. This situation is illustrated in Fig. 3:

$$\psi_j=\sum_{\substack{s=e,h\\ d=f,b}}\phi^j_{s,d} \ , \tag{4.1}$$

$$\phi^j_{e,f}=\begin{bmatrix} a_j \\ 0 \end{bmatrix}\exp[iq^+x](x\in\text{branch } j=0,1,2) \tag{4.1a}$$

$$\phi^j_{e,b}=\begin{bmatrix} b_j \\ 0 \end{bmatrix}\exp[-iq^+x] \quad (x\in\text{branch } j=0,1,2) \tag{4.1b}$$

$$\phi^j_{h,f}=\begin{bmatrix} 0 \\ \tilde{b}_j \end{bmatrix}\exp[-iq^-x] \quad (x\in\text{branch } j=0,1,2) \tag{4.1c}$$

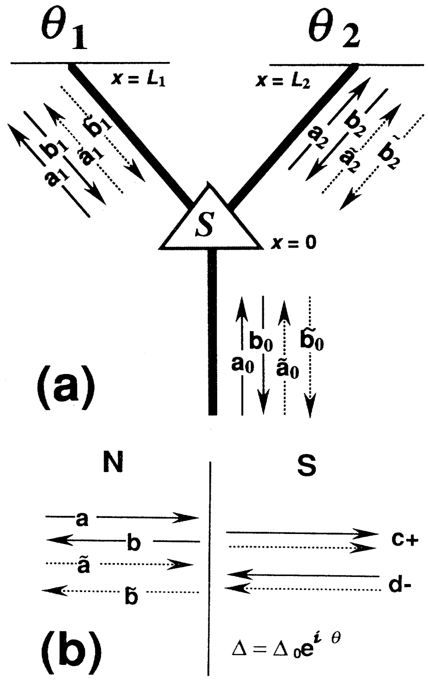

FIG. 3. (a) The model of analysis. 12 waves in the normal-electron waveguide branches are coupled by the scattering matrix **S**. (b) Andreev reflection and the normal reflection are obtained from the boundary condition at the SN interface.

$$\phi^j_{h,b}=\begin{bmatrix} 0 \\ \tilde{a}_j \end{bmatrix}\exp[iq^-x](x\in\text{branch } j=0,1,2) \tag{4.1d}$$

where

$$q^{\pm}=(2m/\hbar^2)^{1/2}(E_F\pm E)^{1/2} \ . \tag{4.2}$$

The subscripts e and h refer to the electron wave and the hole wave, respectively. In Fig. 3(a), electron waves are expressed by solid lines, and hole waves by dashed lines.

These 12 waves are coupled through the 3×3 scattering matrix **S** at the Y-junction point.[12]

$$b_0=S_{00}a_0+\sum_{\alpha=1,2}S_{0\alpha}b_\alpha \ , \tag{4.3a}$$

$$a_j=S_{j0}a_0+\sum_{\alpha=1,2}S_{j\alpha}b_\alpha \quad (j=1,2) \ , \tag{4.3b}$$

$$\tilde{b}_0=S_{00}\tilde{a}_0+\sum_{\alpha=1,2}S_{0\alpha}\tilde{b}_\alpha \ , \tag{4.3c}$$

$$\tilde{a}_j=S_{j0}\tilde{a}_0\sum_{\alpha=1,2}S_{j\alpha}\tilde{b}_\alpha \quad (j=1,2) \tag{4.3d}$$

$$S_{\alpha\beta}=\begin{bmatrix} \sqrt{1-2|T|^2} & T & T \\ T & \rho & \tau \\ T & \tau & \rho \end{bmatrix} \quad (\alpha,\beta=0,1,2) \tag{4.4}$$

where T is the transmission coefficient across branches 0 and 1, or 0 and 2, and τ is that across 1 and 2, and ρ is the reflection coefficient of branches 1 and 2. On the other hand, in the superconducting electrodes, the wave functions with the incident energy within the superconducting gap are evanescent Bogoliubov quasiparticles and are given by

$$\psi_{Si}=\sum_{s=e,h}\gamma_s^i\ , \tag{4.5}$$

where

$$\gamma_e^i=c_{i+}\begin{bmatrix}1\\ X_i\end{bmatrix}\exp[(ik-k_d)(x-L_i)]$$

$$(x\in\text{superconducting electrode } i=1,2)\ , \tag{4.5a}$$

$$\gamma_h^i=d_{i-}\begin{bmatrix}Y_i\\ 1\end{bmatrix}\exp[(-ik-k_d)(x-L_i)]$$

$$(x\in\text{superconducting electrode } i=1,2)\ , \tag{4.5b}$$

and L_i is the length of the branch $i(=1,2)$,

$$k=(2m_s/\hbar^2)^{1/2}E_{Fs}^{1/2}\ , \tag{4.6}$$

$$k_d=(2m_s/\hbar^2)^{1/2}\left[\frac{\Delta_0^2-E^2}{4E_{Fs}}\right]^{1/2}\ , \tag{4.7}$$

$$X_i=(E-i\sqrt{\Delta_0^2-E^2})/\Delta_i=e^{-i(\varphi+\theta_i)}\ , \tag{4.8a}$$

$$Y_i=\Delta_i/(E+i\sqrt{\Delta_0^2-E^2})=e^{-i(\varphi-\theta_i)}\ , \tag{4.8b}$$

φ is the same as in Eq. (2.5), and $\Delta_i=\Delta_0e^{i\theta_i}$ are the pair potentials of the electrodes i. Here, m_s and E_{Fs} are the effective mass and the Fermi energy in the superconductor. γ_e^i is the electronlike Bogoliubov quasiparticle and γ_h^i is the holelike Bogoliubov quasiparticle.

The boundary conditions, which couple the quasiparticle and Bogoliubov quasiparticle, must be satisfied at the SN interfaces between a waveguide branch and a superconducting electrode. Here we consider two types of SN interfaces by taking into account the normal reflection at the interface as well as the Andreev reflection.

First consider an interface where normal reflection occurs because of the wave-number discrepancy between the normal region and the superconducting region, that is, $q\neq k$. For this interface, the boundary condition is

$$(\psi_i-\psi_{Si})|_{x=L_i}=0 \tag{4.9a}$$

and

$$\frac{\partial}{\partial x}(\psi_i-\psi_{Si})|_{x=L_i}=0\ . \tag{4.9b}$$

In the approximation $\Delta_0\ll E_{Fs}$, this compels the waves in branch i to obey the relations as follows:

$$X_i(Q+1)e^{iq^+L_i}a_i+X_i(Q-1)e^{-iq^+L_i}b_i$$
$$-(Q+1)e^{iq^-L_i}\tilde{a}_i-(Q-1)e^{-iq^-L_i}\tilde{b}_i=0\ , \tag{4.10a}$$

$$(Q-1)e^{iq^+L_i}a_i+(Q+1)e^{-iq^+L_i}b_i$$
$$-Y_i(Q-1)e^{iq^-L_i}\tilde{a}_i-Y_i(Q+1)e^{-iq^-L_i}\tilde{b}_i=0\ , \tag{4.10b}$$

where $Q=|k|/|q|$.

At the other type of interface, normal reflection occurs because of the existence of the Schottky barrier at the interface. In this case we think that parameters such as wave numbers and effective mass are the same in the normal and superconducting regions.

Suppose there is a δ-function-like barrier with height H_i. From the boundary condition, Eq. (4.9a) and

$$\frac{\partial}{\partial x}(\psi_i-\psi_{Si})|_{x=L_i}=\frac{2m}{\hbar^2}H_i\psi_i|_{x=L_i}\ , \tag{4.11}$$

we get

$$X_i(1-iZ_i)e^{iq^+L_i}a_i-iZ_iX_ie^{-iq^+L_i}b_i$$
$$-(1-iZ_i)e^{iq^-L_i}\tilde{a}_i+iZ_ie^{-iq^-L_i}\tilde{b}_i=0\ , \tag{4.12a}$$

$$iZ_ie^{iq^+L_i}a_i+(1+iZ_i)e^{-iq^+L_i}b_i$$
$$-iZ_iY_ie^{iq^-L_i}\tilde{a}_i-Y_i(1+iZ_i)e^{-iq^-L_i}\tilde{b}_i=0\ , \tag{4.12b}$$

where $Z_i=H_im/k\hbar^2$.

Solving Eqs. (4.3) and (4.10), or Eqs. (4.3) and (4.12) simultaneously for $a_j,b_j,\tilde{a}_j,\tilde{b}_j$ under the condition $a_0=1$, $\tilde{b}_0=0$, we obtain the Andreev-reflection coefficient $\tilde{a}_0$ and the normal reflection coefficient b_0. The conductance across Q-P is then given by

$$G_{QP}=\frac{2e^2}{h}(1+\tilde{a}_0^*\tilde{a}_0-b_0^*b_0) \tag{4.13a}$$

$$=\frac{4e^2}{h}\tilde{a}_0^*\tilde{a}_0 \tag{4.13b}$$

using the Landauer formula.[13] Here, we used the probability conservation law

$$\tilde{a}_0^*\tilde{a}_0+b_0^*b_0=1\ . \tag{4.14}$$

B. Zero-bias voltage ($V_{QP}=0$) cases

It is very easy to obtain numerically the Andreev-reflection coefficient. However, we find the roots analytically in order to discuss the behavior of the interferometer. The analytical calculation is straightforward but troublesome. We show the results only for some simple but important cases.

For symmetric configurations with $L_1=L_2=L$, $H_1=H_2=H$, considering a zero-bias ($V_{QP}=0$, that is, $E=0$) case. The conductance G is given by

$$G(\theta_1-\theta_2,Q)=\frac{2e^2}{h}\frac{|A_Q(Q)|^2[1+\cos(\theta_1-\theta_2)]}{|D_{Q1}(Q)+D_{Q2}(Q)\cos(\theta_1-\theta_2)|^2}\ , \tag{4.15}$$

for normal reflection by the wave-number discrepancy, and

$$G(\theta_1-\theta_2,Z)=\frac{2e^2}{h}\frac{|A_A(Z)|^2[1+\cos(\theta_1-\theta_2)]}{|D_{Z1}(Z)+D_{Z2}\cos(\theta_1-\theta_2)|^2}\ , \tag{4.16}$$

for normal reflection by the Schottky barrier. Here

$$A_Q(Q)=4QT^2[(Q^2-1)e^{-2iqL}+(Q^2-1)(\rho-\tau)^2e^{+2iqL}+2(Q^2+1)(\rho-\tau)]\ ,$$

$$\begin{aligned}D_{Q1}(Q)=&-(Q^2-1)^2\sqrt{1-2|T|^2}e^{-4iqL}-(Q^2-1)^2(\rho-\tau)^2(\rho+\tau)\{-2T^2+\sqrt{1-2|T|^2}(\rho+\tau)\}e^{+4iqL}\\&+2(Q^4-1)(T^2-2\rho\sqrt{1-2|T|^2})e^{-2iqL}\\&+2(Q^4-1)(\rho-\tau)(3T^2\rho-2\rho^2\sqrt{1-2|T|^2}+T^2\tau-2\rho\tau\sqrt{1-2|T|^2})e^{+2iqL}\\&+2\{\rho(T^2-\rho\sqrt{1-2|T|^2})(3Q^4+2Q^2+3)-\tau(T^2-\tau\sqrt{1-2|T|^2})(Q^2+1)^2\}\ ,\end{aligned}$$

$$D_{Q2}(Q)=-8Q^2\tau(T^2-\tau\sqrt{1-2|T|^2})\ ,$$

$$A_Z(Z)=2T^2[-iZ(1+iZ)e^{-2iqL}+iZ(1-iZ)(\rho-\tau)^2e^{+2iqL}+(1+2Z^2)(\rho-\tau)]\ ,$$

$$\begin{aligned}D_{Z1}(Z)=&2Z^2(1+iZ)^2\sqrt{1-2|T|^2}e^{-4qiL}+2Z^2(1-iZ)^2(\rho-\tau)^2(\rho+\tau)\{-2T^2+\sqrt{1-2|T|^2}(\rho+\tau)\}e^{+4iqL}\\&-2iZ(1+iZ)(1+2Z^2)(T^2-2\rho\sqrt{1-2|T|^2})e^{-2iqL}\\&+2iZ(1-iZ)(1+2Z^2)(\rho-\tau)(3T^2\rho-2\rho^2\sqrt{1-2|T|^2}+T^2\tau-2\rho\tau\sqrt{1-2|T|^2})e^{+2iqL}\\&+2\rho(T^2-\rho\sqrt{1-2|T|^2})(6Z^4+6Z^2+1)-\tau(T^2-\tau\sqrt{1-2|T|^2})(4Z^4+4Z^2+1)\ ,\end{aligned}$$

and

$$D_{Z2}=-\tau(T^2-\tau\sqrt{1-2|T|^2})\ .$$

When $|D_{Z1}(Z)|\gg|D_{Z2}|$ or $|D_{Q1}(Q)|\gg|D_{Q2}(Q)|$ is satisfied, the dependence of the conductance G on the phase difference is similar to $1+\cos(\theta_1-\theta_2)$, as was claimed in the previous section. This occurs for a resistive Y junction. In fact, for $|T|^2\ll1$, $|\tau|^2\ll1$, Eqs. (4.15) and (4.16) reduce to

$$G(\theta_1-\theta_2,Q)=\frac{2e^2}{h}\frac{4|T|^4Q^2[1+\cos(\theta_1-\theta_2)]}{[Q^2+1+(Q^2-1)\cos2qL+O(\tau^2)\cos(\theta_1-\theta_2)]^2} \tag{4.17}$$

and

$$G(\theta_1-\theta_2,Z)=\frac{2e^2}{h}\frac{|T|^4[1+\cos(\theta_1-\theta_2)]}{[(1+2Z^2)+2Z\sin2qL+2Z^2\cos2qL+O(\tau^2)\cos(\theta_1-\theta_2)]^2}\ . \tag{4.18}$$

These $1+\cos(\theta_1-\theta_2)$ dependency breakdown only for the cases when

$$(1+2Z^2)+2Z\sin2qL+2Z^2\cos2qL\simeq0 \tag{4.19}$$

or

$$Q^2+1+(Q^2-1)\cos2qL\simeq0\ . \tag{4.20}$$

These exactly correspond to the condition that a bound state is formed in a branch of the Y junction.

C. Finite voltage ($V_{QP}\neq0$) case

So far we have considered only the cases when $V_{QP}=0$, that is, the incident energy of a quasiparticle is infinitesimal. We are also curious about how the behavior of the interferometer changes with the incident energy. When the incident energy $E=eV_{QP}$ is finite, the result of the analytical calculation is very complex. Here, we show the result for the normal reflection-free case only. The conductance is given by

$$G(\theta_1-\theta_2,E)=\frac{2e^2}{h}\frac{|A_E(E)|^2[1+\cos(\theta_1-\theta_2)]}{|D_{E1}(E)+D_{E2}\cos(\theta_1-\theta_2)|^2}\ , \tag{4.21}$$

where

$$A_E(E)=4T^2(\tau-\rho)\sin(\delta qL-\varphi)\ ,$$

$$\begin{aligned}D_{E1}(E)=&-2\rho(T^2-\rho\sqrt{1-2|T|^2})\\&+e^{i2(\delta qL-\varphi)}(\tau^2-\rho^2)\sqrt{1-2|T|^2}\\&+e^{-i2(\delta qL-\varphi)}\{(\tau^2-\rho^2)\sqrt{1-2|T|^2}\\&+2T^2(\rho-\tau)\}\ ,\end{aligned}$$

$$D_{E2}=2\tau(T^2-\tau\sqrt{1-|T|^2})\ ,$$

and $\delta q=q^+-q^-$.

In this case, the analogous condition to Eqs. (4.19) and (4.20) for the formation of a bound state is

$$1+\cos2(\delta qL-\varphi)\simeq0\ . \tag{4.22}$$

The existence of the phase factor $e^{\pm i2(\delta qL-\varphi)}$ in the denominator of Eq. (4.21) makes the dependence on the phase difference more subtle than in the zero-bias case. We provide an example of this curious behavior in the next section.

V. RESULTS AND DISCUSSION

A. Effect of the normal reflection at the SN interface

We now show the results of the calculations in the previous section. In all the calculations we used the parameters

$$T=\tau=\frac{1}{\sqrt{3}}\exp[i2\pi/3]\ ,\quad \rho=\sqrt{1-2|T|^2}=1/\sqrt{3}\ , \tag{5.1}$$

and $qL=9.5$.

The conductances across Q-P for various normal reflection intensities calculated from Eq. (4.15) are shown in Fig. 4. In this case, normal reflection occurs because of the discrepancy between the wave numbers across the SN interface. As expected, the absolute value of the conductance decreases when the normal reflection at the SN interface becomes stronger, that is, for larger Q. The dependence on phase difference is important for the interferometer behavior rather than the absolute value of the conductance. The conductances take maximal values at $\theta_1-\theta_2=0$. We call this type of dependence "upward convex" (UC) and the opposite type of dependence which takes the minimal value there is called "downward convex" (DC).

A large relative change of conductance as the function of the phase difference is favorable to the interferometer. When there is no normal reflection at the SN interface ($Q=1$), the dependence on phase difference is weaker than $1+\cos(\theta_1-\theta_2)$ expected from Sec. III. How does the normal reflection affect this dependence? In order to investigate this, conductance normalized by its value at $\theta_1-\theta_2=0$ is shown in Fig. 5. The dependence on phase difference is clearer for large Q. First thoughts suggest that this is strange because only the Andreev-reflected component is affected by the macroscopic phase and the normal reflected component is not, considering the principle described in Sec. III. This is one of the faults of the primitive discussion in that section. When the resistive properties of the Y junction are taken into account, as is in Sec. IV, the Andreev-reflected and normal reflected components combine through the normal reflection at the Y-junction point. Therefore, both of them take part in the dependence of the interference on macroscopic phase difference.

Figure 6 shows the same properties as Fig. 5 for the case when normal reflection occurs by the Schottky barrier, calculated from Eq. (4.16). For large Z, the behavior is similar to that in Fig. 5 with the relationship $Z^2\leftrightarrow Q$.

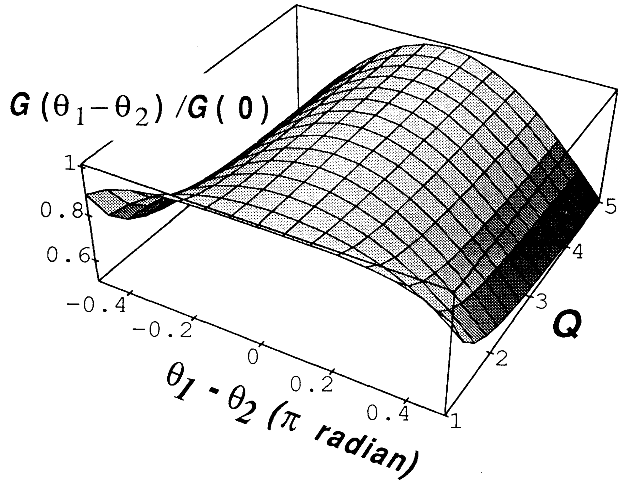

FIG. 5. The dependence of the normalized conductance across Q-P on the phase difference vs the intensity of the normal reflection at the SN interface. This is for normal reflections due to the wave-number discrepancy between the normal waveguide and the superconducting electrode: $Q=|k|/|q|$ ($V_{QP}=0$).

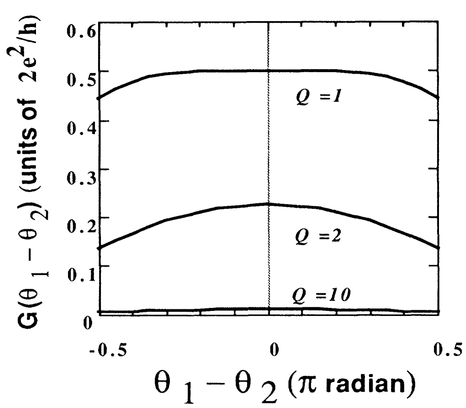

FIG. 4. The absolute value of the conductance across Q-P and its dependence on the phase difference under various normal reflection intensities. Q is a parameter which expresses the wave-number discrepancy between the normal waveguide and the superconducting electrode: $Q=|k|/|q|$ ($V_{QP}=0$).

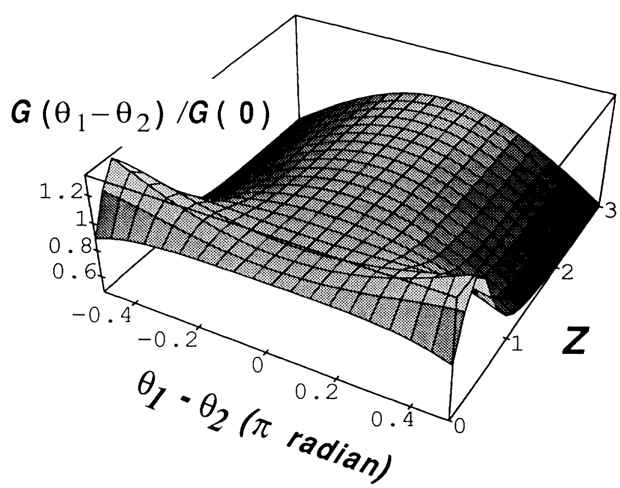

FIG. 6. The dependence of the normalized conductance across Q-P on the phase difference vs the intensity of the normal reflection at the SN interface. This is for normal reflections due to the existence of the Schottky barrier between the normal waveguide and the superconducting electrode: $Z=Hm/k\hbar^2$ ($V_{QP}=0$).

The dependence on phase difference in the vicinity of $Z=0.5$ is curious. Although UC dependence is expected from the discussion in Sec. III, we find DC dependence in this region. This is a typical example that satisfies the condition of Eq. (4.19) and shows that the behavior of the interferometer is different depending on the origin of normal reflection. As noted above, the formation of a state nearly bounded in a waveguide branch by the reflections at the Y-junction point and the SN interface causes this DC dependence. Therefore, the analysis in Sec. III, which neglected the normal reflection at the Y-junction point did not give this type of dependence. Since each branch of the interferometer is an open system, there is no exact bound state. For convenience, we call the state which approximately satisfies the condition of the bound-state formation, a bound state.

B. Dependence on energy for the interferometer

Next, we look at the non-zero-bias voltage cases such that $V_{QP}\neq 0$, that is, the incident energy E of a quasiparticle is finite. The result of the calculation for the normal reflection-free case from Eq. (4.21) is shown in Fig. 7(a).

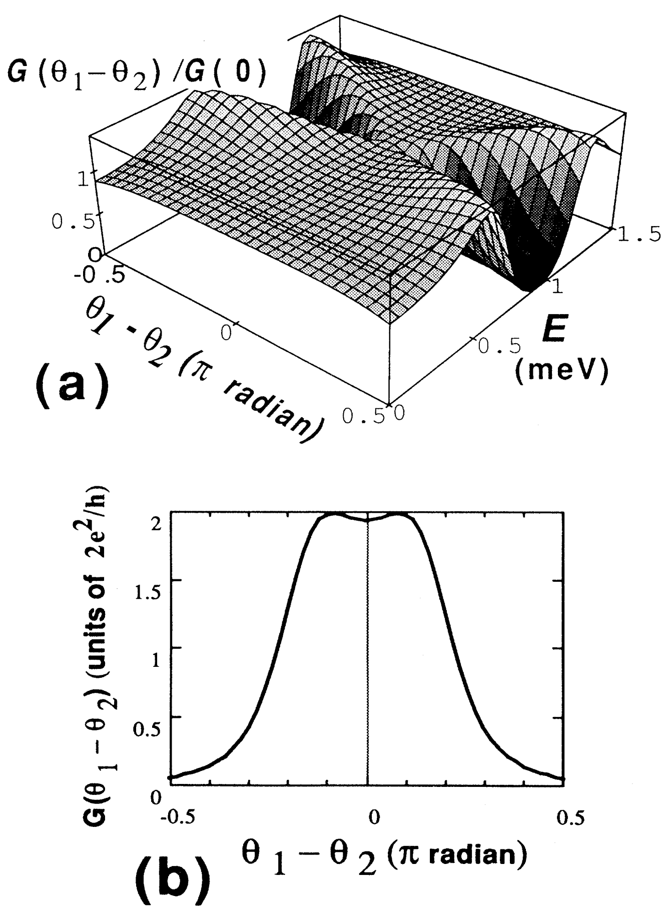

FIG. 7. (a) The dependence of the normalized conductance across Q-P on the phase difference vs the incident energy E with a superconducting gap energy $\Delta_0=1.5$ meV. This is for the case where there is no normal reflection at the SN interface. (b) The cross section at $E=1.0$ meV.

Here we used additional parameters such as the Fermi energy in the waveguide $E_F=10$ meV, the effective mass of the electron $m=0.05m_0$, where m_0 is the free-electron mass, and the superconducting gap energy $\Delta_0=1.5$ meV. The dependence on E near $E=1.0$ meV is rather complicated. With an increase in energy, the dependence on the phase difference shows DC behavior and suddenly changes into a UC type, and then returns to DC. This is quite different from the zero-bias voltage cases where the formation of a bound state in a waveguide branch always causes dependency on phase difference with a DC shape. From Eq. (4.22), we know that, for the present parameters, there exists only one bound state in a waveguide branch in this energy region (from 0 to Δ_0). Also the bound state is positioned in the vicinity of $E=1.0$ meV. The strong UC dependency in Fig. 7(b) is attributed to the cancellation between $D_{E1}(E)$ and $D_{E2}\cos(\theta_1-\theta_2)$ in Eq. (4.21) near $\theta_1-\theta_2=0$. This never occurs in Eq. (4.17) for normal reflection by the wave-number discrepancy or in Eq. (4.18) for reflection by the Schottky barrier in the zero-bias voltage case. This behavior suggests the possibility of better operation of the interferometer by tuning the incident energy, that is, the bias voltage.

C. Asymmetric configuration and multimode effects

The above discussion is based on the analysis for the single-mode waveguide in Sec. IV. Here we comment on the effects which occur with multimode transmission along the waveguide.

When observing the Aharonov-Bohm effect,[14] in metal rings, the aspect ratio of the rings is very important. Although a waveguide wider than the Fermi wavelength has many transmission modes which experience different phase advances, the modes do not modify the interference effect if the aspect ratio is large enough.[15] The superposition of the modes, however, modifies the behavior of the interference to be more complex. In fact, the experiment by Webb *et al.*[15] needed the Fourier transform to identify the origin of the interference. In our interferometer the phase shift by Andreev reflection and the phase advance along the propagation is independent of the incidence angle of the quasiparticle owing to the retroactive property of the Andreev-reflected particle. In other words, all modes in the waveguide are phase-shifted by the same amount, as noted in Sec. III. Therefore, the average of the modes does not modify the interference effect if the normal reflection at the SN interface can be neglected. Therefore, it would be possible to observe the interference effect more directly than Aharonov-Bohm experiments.

Even in the presence of normal reflections, if the interferometer has a symmetric configuration, no problem occurs. In an asymmetric configuration, however, the interferometer suffers from destructive influences by two nonretroactive phenomena. The first is the normal reflection which forms a different standing-wave-like state in each waveguide. This moves the phase-difference value where the conductance takes its extreme value. Since the shift is different for every mode, too many transmission modes act destructively in the interferometer. Therefore, it is desirable to make the waveguide of a material with a long Fermi wavelength. The second destructive influence is due to the finite incident energy $E=eV_{QP}$. From Eq. (2.3) the imperfection of the retroactive property of an Andreev-reflected hole is given by

$$\delta q \sim \left[\frac{2m}{\hbar^2}\right]^{1/2} \frac{E}{(E_F-E_\perp)^{1/2}} . \quad (5.2)$$

If $\delta q \delta L$ is comparable to π, the imperfection of the retroactive property is not negligible, where δL is the asymmetry of the two waveguide branches. This limits the bias voltage V_{QP} in order to achieve the proper operation of the interferometer. An example value is estimated in the next subsection.

D. Feasible materials for the interferometer

Consider the materials and dimensions necessary for this interferometer. The electron waveguide must be made of a material with high mobility and long phase coherence length L_ϕ. A degenerate semiconductor is suitable from the viewpoint of fabrication and its long Fermi wavelength. Taking into account the limits of fabrication techniques, the length of the waveguide branch L is reasonable at a few μm. Since a low temperature is already required in order to get a long L_ϕ waveguide, a Josephson junction composed of high-T_c superconductors is not necessary.

For example, the combination of n-doped InAs and Nb is a hopeful candidate. The InAs-Nb interface is Schottky barrier free and it gives a large Andreev-reflection probability,[16] that is, small intrinsic normal reflection. Since it is difficult to fabricate a perfect single-mode waveguide, it is better to avoid normal reflection if possible, as was discussed above. Moreover, n-doped InAs has a rather long L_ϕ. At a few K, L_ϕ is over a few μm for samples with carrier density $n \sim 10^{18}$ cm^{-3}.[17]

As mentioned above, the asymmetry between the two waveguide branches limits the applied voltage across Q-P for the proper operation of the interferometer. When δL is of submicron order, δq needs to be less than 10^5 m^{-1}. For the case of InAs with $n=10^{18}$ cm^{-3} and Nb with $\Delta_0=1.5$ meV, from Eq. (5.2), V_{QP} should be limited to below one-tenth of the superconducting gap voltage of Nb.

E. Self-generated magnetic flux

Our last point in this section is that the magnetic field generated by the supercurrent flowing through the JJ is negligible for quasiparticle interference. The magnetic flux piercing the area enclosed by the JJ and the Y branches causes a shift in the phase of normal electrons or holes in the waveguide, as occurs in the Aharonov-Bohm effect. This effect might hinder the observation of the phase shift by Andreev reflection. The magnetic flux is estimated to be of the order of $\mu_0 I_s g L$, where μ_0 is the permeability of a vacuum, and g is a geometrical factor of the order of unity. When the length of branch L is a few μm, and the supercurrent is a few μA, the flux is about $10^{-4}h/e$. Therefore, the phase shift caused by the magnetic flux is negligible.

VI. CONCLUSION

We proposed a quasiparticle interferometer which enables us to experimentally confirm the interaction between the microscopic phase of a quasiparticle and the macroscopic phase of a superconducting state due to Andreev reflection at the SN interface. The interferometer consists of a Y-type junction composed of normal-electron waveguides and a Josephson junction, and the modification of the interference by the bias supercurrent of the Josephson junction affects the resistance of the normal-electron waveguide. We also gave a quantitative analysis of the interferometer, which considered the characteristics of the Y junction and the normal reflection at the SN interface. Although the normal reflection is not necessarily destructive to the operation of the interferometer, it often makes the behavior complicated. Moreover, the bias voltage applied to the waveguide affects the behavior of the interferometer. This suggests the possibility of better operation of the interferometer by tuning the bias voltage.

ACKNOWLEDGMENTS

We are indebted to S. Takagi of Tohoku University for his helpful suggestions. We wish to thank N. Hatakenaka, S. Kurihara, and J. Nitta of NTT for fruitful discussions and H. Hiratsuka and T. Kimura of NTT for their encouragement through this work.

[1]For reviews, see articles in *Mesoscopic Phenomena in Solids*, edited by B. L. Altshuler, P. A. Lee, and R. A. Webb (North-Holland, Amsterdam, 1991).

[2]T. Van Duzer and C. W. Turner, *Principles of Superconductive Devices and Circuits* (Elsevier–North-Holland, New York, 1981), and references therein.

[3]A. F. Andreev, Zh. Eksp. Teor. Fiz. **46**, 1823 (1964) [Sov. Phys. JETP **19**, 1228 (1964)].

[4]B. Z. Spivak and D. E. Khmel'nitskiĭ, Pis'ma Zh. Eksp. Teor. Fiz. **35**, 334 (1982) [JETP Lett. **35**, 412 (1982)].

[5]H. Nakano and H. Takayanagi, Solid State Commun. **80**, 997 (1991); H. Nakano and H. Takayanagi, in *Science and Technology of Mesoscopic Structures*, Proceedings of the International Symposium, Nara, 1991, edited by S. Namba, C. Hamaguchi, and T. Ando (Springer-Verlag, Tokyo, 1992).

[6]P. G. de Gennes, Rev. Mod. Phys. **36**, 225 (1964); *Superconductivity of Metals and Alloys* (Benjamin, New York, 1966).

[7]G. E. Blonder, M. Tinkham, and T. M. Klapwijk, Phys. Rev. B **25**, 4515 (1982).

[8]B. L. Altshuler, D. E. Khmelnitskii, and B. Z. Spivak, Solid State Commun. **48**, 841 (1983).

[9]B. L. Al'tshuler and B. Z. Spivak, Zh. Eksp. Teor. Fiz. **92**, 609

(1987) [Sov. Phys. JETP **65**, 343 (1987)].
[10]M. Büttiker and T. M. Klapwijk, Phys. Rev. B **33**, 5114 (1986).
[11]B. D. Josephson, Phys. Lett. **1**, 251 (1962).
[12]S. Takagi, Solid State Commun. **81**, 579 (1992).
[13]R. Landauer, IBM J. Res. Develop. **1**, 223 (1957); Philos. Mag. **21**, 863 (1970).
[14]Y. Aharonov and D. Bohm, Phys. Rev. **115**, 485 (1959).
[15]R. A. Webb, S. Washburn, C. P. Umbach, and R. B. Laibowitz, Phys. Rev. Lett. **54**, 2696 (1985).
[16]J. Nitta, H. Nakano, T. Akazaki, and H. Takayanagi, in *Single-Electron Tunneling and Mesoscopic Devices,* edited by H. Koch and H. Lübbig (Springer-Verlag, Heidelberg, 1992).
[17]H. Nakano, T. Akazaki, J. Nitta, and H. Takayanagi, Solid State Commun. **80**, 251 (1991).